Structural location of the iron ions in cordierite: A spectroscopic study

Article *in* Contributions to Mineralogy and Petrology · July 2001

DOI: 10.1007/s004100100234

3 authors, including:

Vladimir M. Khomenko
National Academy of Sciences of Ukraine
52 PUBLICATIONS **469** CITATIONS

SEE PROFILE

Charles A. Geiger
University of Salzburg
245 PUBLICATIONS **4,302** CITATIONS

SEE PROFILE

Contrib Mineral Petrol (2001) 141: 381–396
DOI 10.1007/s004100100234

Vladimir M. Khomenko · Klaus Langer
Charles A. Geiger

Structural locations of the iron ions in cordierite: a spectroscopic study

Received: 27 June 2000 / Accepted: 28 November 2000 / Published online: 3 May 2001

Abstract A series of 21 cordierites with $0.06 < Fe^{2+}$ cations pfu < 1.54 from different petrogenetic environments were studied by polarized electronic absorption single-crystal spectroscopy and ^{57}Fe Mössbauer spectroscopy (MS). The electronic spectra measured in the range 35,000–1,000 cm^{-1} using microscope techniques were also obtained at different temperatures between 80 and 700 K on five different samples. The aim of this study was to answer the still-debated question of the location of iron in the cordierite structure. Both electronic absorption and ^{57}Fe Mössbauer spectra confirm the presence of Fe^{2+} on two different structural positions. The major fraction, 90–99% of the total Fe^{2+}, occupies the octahedral site 8*g* in orthorhombic cordierite. Minor amounts of Fe^{2+} occur in a second, non-octahedral site. The octahedral and non-octahedral Fe^{2+} give rise to two MS doublets and to different absorption bands in the electronic absorption spectra, namely v_1 and v_2 at about 8,300 and 10,000 cm^{-1} both of which are α-polarized for octahedral Fe^{2+}, and β/γ-polarized v_3 at about 10,500 cm^{-1} for non-octahedral Fe^{2+}. The integral intensities of the v_1 and v_2 bands increase linearly with increasing total iron contents. Their energies decrease slightly with increasing Fe^{2+}. Increasing temperature causes a shift of v_1 to lower energies, while the integral intensities of v_1 and v_2 increase. These observations permit an assignment of the v_1 and v_2 bands to transitions derived from the $^5T_{2g} \rightarrow {}^5E_g$ transition of octahedral Fe^{2+}. The integral intensity of the β- and γ-polarized v_3 band correlates linearly with the concentration of non-octahedral Fe^{2+}. Its high molar extinction coefficient, ca. 150 cm^{-2} l mol^{-1}, and temperature independence are best explained by its assignment to *dd* transitions of Fe^{2+} in tetrahedral coordination. There occurs also a broad band at 18,000 cm^{-1} polarized predominantly along *b*. Its properties are typical of a metal–metal charge transfer (CT) band involving Fe^{2+} on the octahedra and Fe^{3+} on the $T_1$1-tetrahedra, the two of which are edge-shared. All spectroscopic data, including changes in the electronic spectra caused by heating at 1,000 °C in air, as well as crystal-chemical considerations, suggest that the ring-connecting $T_1$1-tetrahedra contain small amounts of Fe^{2+}.

V.M. Khomenko (✉)
Institute of Geochemistry, Mineralogy and Ore Formation,
Ukrainian Academy of Science, pr. Palladina 34,
252142 Kyiv, Ukraine

K. Langer
Institut für Angewandte Geowissenschaften I,
Allgemeine und Experimentelle Mineralogie,
Technische Universität Berlin, Ernst-Reuter-Platz 1,
10623 Berlin, Germany

C.A. Geiger
Institut für Geowissenschaften, Universität Kiel,
Olshausenstr. 40, 24098 Kiel, Germany

V.M. Khomenko
Present address:
Institut für Angewandte Geowissenschaften
I, Allgemeine und Experimentelle Mineralogie,
Technische Universität Berlin, Ernst-Reuter-Platz 1,
10623 Berlin, Germany,
e-mail: vladkhom@hotmail.com
Tel.: +49-30-31425162; Fax: +49-30-31421124

Editorial responsibility: J. Hoefs

Introduction

The structural location and valence state of the iron ions in cordierite are of interest to mineralogists and ceramists. They are important because of their effect on thermodynamic calculations, their possible influence on the low thermal expansion of cordierite, their role in the origin of the spectacular pleochroism of the mineral, and, finally, because of their significance in explaining the crystallochemical features of a variety of silicate structures possessing infinite channels formed by the stacking of six-membered (Si, Al) tetrahedral rings.

Cordierite is a framework aluminosilicate with the general formula $(Mg, Fe)_2Al_4Si_5O_{18}{\cdot}n(H_2O, CO_2)$. It is common in low- and medium-pressure metapelitic rocks of amphibolite and granulite facies. The crystal structure

(Gibbs 1966) of most natural cordierites is orthorhombic of space group *Cccm* with four formula units per unit cell. It contains distorted six-membered corner-shared tetrahedra rings. The tetrahedra have centres at the Wycoff position 8*l* of site symmetry *m*, but with different atomic coordinates giving two pairs of $T_2$3 and $T_2$1 Si-tetrahedra and two $T_2$6 Al-tetrahedra (Fig. 1a, the labelling of the sites follows Hochella et al. 1979). The rings are stacked over each other along [001] and interconnected by $T_1$1 Al-tetrahedra on 8*k* of site symmetry *2*, and Si-tetrahedra $T_1$6, on 4*b* of point symmetry *222* (Fig. 1a, b). The octahedral ions are on the 8*g* position of point symmetry *2*. The stacking of the tetrahedral rings along [001] produces infinite channels parallel to *c*, which can contain atoms and molecules. Two types of channel positions are shown in Fig. 1, Ch0 at 4*a* of point symmetry *222* (Fig. 1b) and Chw at 8*h* of site symmetry *2* (Fig. 1c).

Since Duncan and Johnston (1974) first determined in a Mössbauer study on oriented cordierite crystals that a minor amount of divalent iron is located on a non-octahedral site, there has been ongoing discussion regarding this possible site. Goldman et al. (1977) proposed that a band at 10,500 cm^{-1} in the β- and γ-polarized electronic spectra of cordierite originates from non-octahedral Fe^{2+}. It is accepted that this absorption band and the "non-octahedral" Fe^{2+} doublet in the Mössbauer spectra are a result of a minor Fe^{2+} fraction located on the same structural site. This conclusion is supported by changes in the Mössbauer and electronic spectra observed after heating samples above 500 °C. Both methods show a similar increase in the octahedral to non-octahedral ferrous iron ratio after heating (Vance and Price 1984).

Different sites have been suggested for this minor non-octahedral Fe^{2+} (Duncan and Johnston 1974; Pollak 1976; Goldman et al. 1977; Vance and Price 1984; Geiger et al. 2000a). Two general views exist. One group believes that this Fe^{2+} is located in the channels (Duncan and Johnston 1974; Goldman et al. 1977; see Fig. 1b and c). A second group has proposed a tetrahedral position for this non-octahedral Fe^{2+} (Vance and Price 1984; Geiger et al. 2000a). Although these two kinds of sites are very different crystal-chemically (e.g. Armbruster 1986), the controversial interpretations of the spectroscopic results demonstrate that the experimental data are insufficient for unequivocal conclusions. Additional data, including results on the temperature, polarization and composition behaviour of the electronic absorption bands and Mössbauer spectra, measured on the same set of cordierite samples, are necessary to differentiate between the possible structural locations of the non-octahedral Fe^{2+}.

Although natural cordierites display a range of Fe–Mg substitution and the structure allows other substitutions involving ions of different charges, recent investigations show very low contents of ferric ions (e.g. Geiger et al. 2000a, 2000b). On the other hand, Faye et al. (1968) showed that the impressive violet-blue (β-, γ-polarizations) to orange (α-polarization) pleochroism typical of cordierite, is caused by $Fe^{2+}Fe^{3+}$ CT. Here again, a determination of the site and the concentrations of Fe^{3+} are not possible by standard chemical and X-ray diffraction methods. The main experimental tools that can provide information on these questions are spectroscopic methods, especially single-crystal electronic spectroscopy.

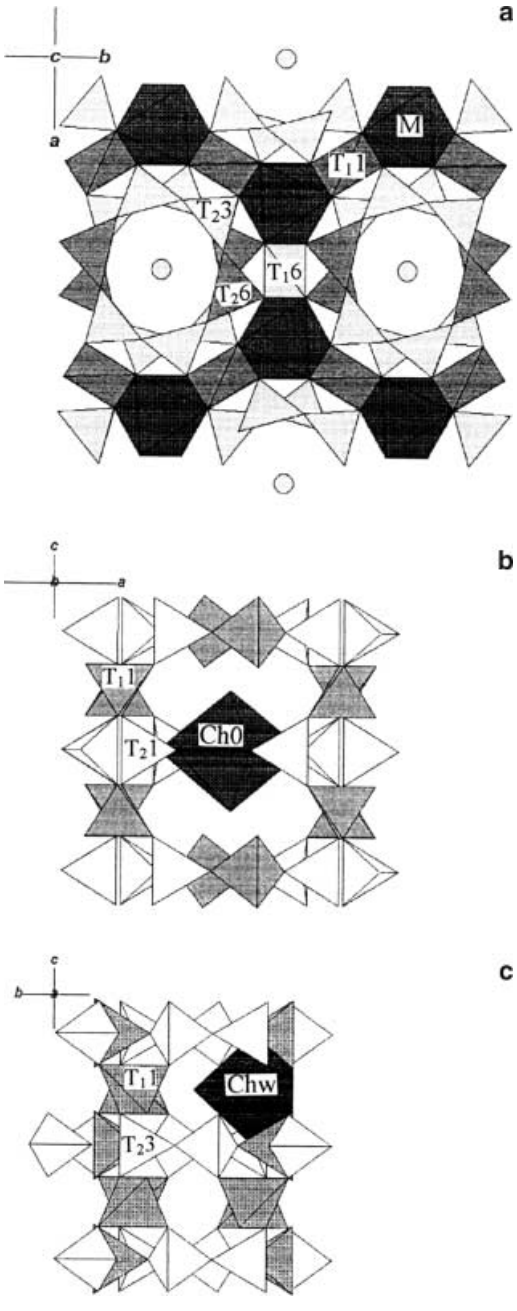

Fig. 1 Sections of the cordierite structure. Possible Fe^{2+}-polyhedra are shown in *black*, the Al-tetrahedra are shaded *grey*. Some tetrahedra are omitted in the projections **b** and **c** for clarity. **a** Structure projection onto (001); **b** channel position (000) in the centre of a six-membered ring; **c** "wall" position in the channel after Duncan and Johnston (1974). The optical polarization directions α, β and γ are parallel to *c*, *b* and *a* respectively

This study was undertaken to determine the site locations of Fe^{2+} and Fe^{3+} in cordierite using a combination of single-crystal electronic (80 K to 700 K) and Mössbauer spectroscopic measurements and crystal-chemical data obtained on a well-characterized series of natural cordierites from different petrologic environments and of different composition.

Experimental methods

Sample description and preparation

Cordierite samples from 21 different localities and rocks types, most of which are described in the literature, were studied using single-crystal electronic absorption and Mössbauer spectroscopic methods. For some samples the PT conditions of formation, based mostly on the garnet–cordierite equilibrium (e.g. Kurepin 1991), are known. These data are summarized in Table 1.

Fragments of cordierite crystals were separated from the rock samples and oriented parallel to (100), (010) and/or (001) using their conoscopic interference figures. Then they were ground and polished on both sides to a thickness of 0.1–0.5 mm. The platelets obtained were used for measurements of the single-crystal polarized electronic spectra and for electron microprobe studies. The latter were performed on those areas on which the electronic spectra were recorded. The compositions are presented in Table 2. The remaining cordierite material was ground into a powder for a measurement of the ^{57}Fe Mössbauer spectra.

Conditions and standards used for the electron microprobe analyses are described in Khomenko et al. (1994) and Langer and Khomenko (1999).

Single-crystal electronic absorption spectroscopy

The polarized spectra with E//*a* (γ-spectra), E//*b* (β-spectra) and E//*c* (α-spectra) were measured at room temperature in the spectral range 35,000–1,000 cm^{-1} by means of a single-beam microscope spectrometer model UMSP 80 from Zeiss (35,000–12,000 cm^{-1}) and a Bruker FTIR spectrometer IFS 66 (13,000–1,000 cm^{-1}) with an IR-microscope attachment. For the Zeiss spectrometer, a 10× Ultrafluars served as the objective and condenser. The measuring diameter was 32 μm, the spectral slit width and step width were both 1 nm. With the FTIR-Bruker spectrometer, equipped with an IR-microscope and polarizer, the polarized spectra were obtained with a measuring diameter of 90 μm and a spectral resolution of 2 cm^{-1}. Further experimental details are given in Langer (1988).

Curve deconvolution of overlapping absorption bands was done with the program OPUS 2.2 using the approach described in Geiger et al. (2000a). Different deconvolutions using the same procedure gave differences in band positions of less than 0.4%. The crystal field parameter Dq was extracted from the spectra using the same estimation of the ground T-level splitting as in Langer and Khomenko (1999).

Five samples, numbers 3, 9, 14, 17 and 21 in Table 1, were chosen for spectroscopic measurement at low (80 K) and high (500 and 700 K) temperatures. These measurements were performed on both spectrometers with an accuracy of ±10 using a Linkam THMS 600 heating–freezing stage equipped with a TP 92 temperature controller. A gold grating placed on the heating–cooling cell served as a sample holder. Reference spectra were measured through the Linkam stage at the same temperature. The scanning and fitting procedures were the same as those of the room-temperature measurements. The temperatures of the crystals could not be measured directly. However, differences between the sample and the heating–freezing cell are probably less than 10 K, which will affect the spectra negligibly.

^{57}Fe Mössbauer spectroscopy

The Mössbauer spectra of 15 cordierites were measured at room temperature and/or 77 K with a nominal 50 mC ^{57}Co/Rh source using a 512 multi-channel analyser. The low-temperature measurements were made with an Oxford cryostat. Cordierite powders were pressed together with corn starch into pellets with approximately 5 mg Fe^{2+} per cm^3. The spectra were fitted to either one or two symmetric doublets with the program MÖSALZ, (W. Lottermoser, personal communication). Isomer shifts are given relative to metallic iron. More details can be found in Geiger et al. (2000a).

Table 1 Cordierite samples studied. *n.d.* Not determined

Number	Sample label	Locality	Rock type	PT estimate	References
1	GRR90	Unknown	n.d.	n.d.	Shannon et al. (1992)
2	Rhodesia	Rhodesia	Metamorphic	n.d.	Geiger et al. (2000a)
3	42/IA	Kiranur, S. India	Granulite	740 ± 40 °C; 7 ± 0.4 kbar	Lal et al. (1984); Geiger et al. (2000a)
4	GR338	Tzilaizina, Madagascar	n.d.	n.d.	Goldman et al. (1977)
5	8c6b/004	Soendeled, Norway	Pegmatite	n.d.	None
6	8c6b/006	Madagascar	n.d.	n.d.	None
7	GR92	Madagascar	n.d.	n.d.	Shannon et al. (1992)
8	56–81	Ivanov, Ukraine	Granite	780 °C; 7 ± 1 kbar	Kurepin (1991)
9	Manitouwadge	Ontario, Canada	Amphibolite	650 ± 30 °C; 6 ± 1 kbar	Pan and Fleet (1995)
10	62–81	Ivanov, Ukraine	Granite	790 °C; 7 ± 1 kbar	Kurepin (1991)
11	1201	Ivanov, Ukraine	Granite	780 °C; 7 ± 0.1 kbar	Kurepin (1991)
12	39–83	Solomin, Ukraine	Granite	730 °C; 6.3 ± 0.2 kbar	Kurepin (1991)
13	Derivo-Colico	Como, Italy	Quartz vein	n.d.	Mottana et al. (1983)
14	VS-2	Colombo, Sri Lanka	Granulite	730 ± 20 °C; 5.2–5.9 kbar	Raase and Schenk (1994)
15	Haddam	Connecticut, USA	Pegmatite	n.d.	Newton (1966); Selkregg and Bloss (1980)
16	66–82	Zhezhelev, Ukraine	Granite	630 °C; 5.2 ± 0.3 kbar	Kurepin (1991)
17	9–81	Sofievka, Ukraine	Pegmatite	600 °C	Kurepin (1991)
18	P-81	Polohov, Ukraine	Pegmatite	n.d.	Voznyak et al. (1996)
19	SN72123	Synder Bay, Canada	Quartzite	665–900 °C; 2.25 kbar	Selkregg and Bloss (1980); Speer (1982)
20	SN72189	Synder Bay, Canada	Quartzite	665–900 °C; 2.25 kbar	Selkregg and Bloss (1980); Speer (1982)
21	Sekaninaite	Dolni Bory, Czech Rep.	Pegmatite	n.d.	Stanek and Miskovsky (1964); Cerný et al. (1997)

Table 2 Chemical composition of cordierites studied (number of atoms per formula unit calculated using 18 O)

Cations/no.	1	2	3	4	5	6	7	8	9	10	11	12	13[a]	14	15[a]	16	17	18[a]	19	20	21[a]
Si	5.00	4.98	4.95	4.99	5.01	4.96	5.00	5.01	5.01	5.03	4.98	5.02	5.00	4.99	5.05	4.98	4.96	5.12	4.96	4.99	4.91
Al	3.97	3.94	3.97	3.97	3.94	4.00	3.97	4.01	3.97	3.97	4.00	3.97	4.00	3.97	3.85	4.01	4.01	3.99	4.01	4.01	4.10
Fe[b]	0.06	0.19	0.21	0.22	0.22	0.24	0.30	0.39	0.41	0.42	0.45	0.50	0.54	0.56	0.57	0.69	0.87	0.89	1.15	1.48	1.54
Mn	n.d.	0.00	0.00	0.00	0.00	0.00	n.d.	0.00	0.00	0.00	0.00	0.00	0.02	0.01	0.04	0.01	0.01	0.04	0.01	0.01	0.07
Mg	1.97	1.90	1.90	1.84	1.78	1.83	1.72	1.56	1.60	1.56	1.60	1.48	1.40	1.48	1.36	1.32	1.15	0.64	0.90	0.51	0.36
Ca	n.d.	0.00	0.00	0.00	0.00	0.00	n.d.	0.00	0.00	0.00	0.00	0.01	0.00	0.00	0.00	0.00	0.00	0.01	0.00	0.00	0.01
Na	0.03	0.07	0.07	0.04	0.12	0.04	0.04	0.01	0.04	0.01	0.01	0.03	0.10	0.01	0.30	0.03	0.08	0.40	0.01	0.01	0.12
K	n.d.	0.00	0.00	0.00	0.00	0.00	n.d.	0.00	0.00	0.00	0.00	0.01	0.00	0.00	0.00	0.00	0.00	0.00	0.00	0.00	0.00
Sum cat.	11.03	11.08	11.10	11.05	11.08	11.06	11.03	10.10	11.03	10.99	11.03	11.01	11.06	11.03	11.30	11.03	11.09	11.09	11.03	11.02	11.11
Fe/(Fe+Mg)	0.03	0.09	0.10	0.11	0.11	0.12	0.15	0.20	0.21	0.21	0.22	0.25	0.28	0.28	0.30	0.34	0.43	0.58	0.56	0.74	0.81
Na+K+Ca	0.03	0.07	0.07	0.04	0.12	0.04	0.04	0.02	0.04	0.01	0.01	0.04	0.10	0.01	0.30	0.03	0.09	0.41	0.01	0.02	0.13

[a]No. 13 contains 0.006 Be (Mottana et al. 1983; no.15 – 0.13 Be (Newton 1966); no.18 – 0.158 Be, 0.096 Li (Vozynak et al. 1996); no.21 – 0.04–0.24 Li, 0–0.003 Be (Černý et al. 1997)
[b]Fe as Fe^{2+}

Results and discussion

Cordierite compositions and crystal-chemical correlations

The compositions of 14 of the 21 cordierites show a slight excess, up to 0.1 atom pfu, of divalent cations (Mg + Fe + Mn) over the stoichiometric value of 2.0. The fraction of such cordierites would be even greater, if two Li-bearing samples were excluded. Such a cation excess is common in natural cordierites. This observation, together with the deficiency in the number of Si + Al + Be cations in tetrahedral sites, taking into account the minor Be and Li in most samples, suggests the following possible substitutions:

$$\square^{T} + Na^{+,Ch} + Fe^{2+,Ch} \leftrightarrow Al^{3+,T} \quad (1)$$

assuming a channel position for minor non-octahedral Fe^{2+} and the presence of tetrahedral vacancies in the structure;

$$(Mg, Fe)^{2+,T} + Na^{+,Ch} \leftrightarrow Al^{3+,T} \quad (2)$$

with divalent cations in tetrahedral sites and Na in the channels; or

$$Si^{4+,T} + (Mg, Fe)^{2+,T} \leftrightarrow 2Al^{3+,T} \quad (3)$$

Energetically, a complete occupancy of framework sites (substitution 2 or 3) should be preferable. A rough negative correlation between non-octahedral Fe^{2+} and the sum of the "tetrahedral" ions (Fig. 2) is consistent with any of the substitutions (1), (2) or (3).

Our compositional data show a negative linear correlation between the sum of the divalent octahedral and the sum of the tetrahedral (Al + Si + Be) cations (Fig. 3). The best-fit line nearly intersects the "stoichiometric" point (Mg + Fe + Mn = 2, Al + Si + Be = 9) and describes well

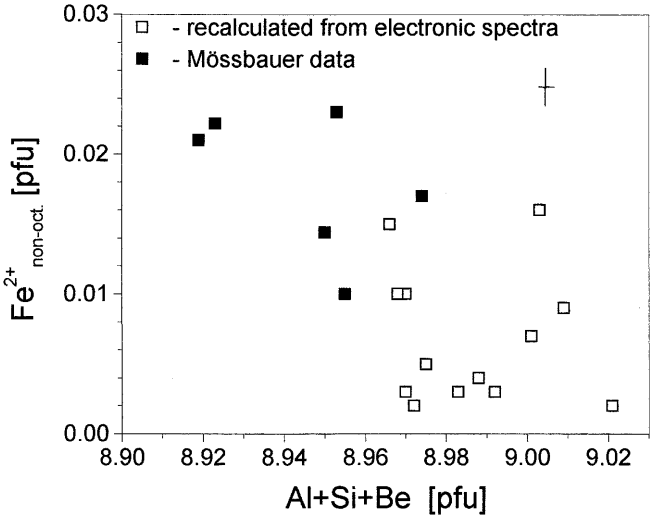

Fig. 2 Content of non-octahedral Fe^{2+} as a function of the sum of the Si + Al + Be tetrahedral cations. An *error bar* is shown for the Mössbauer data. See text for a calculation of non-octahedral Fe^{2+}

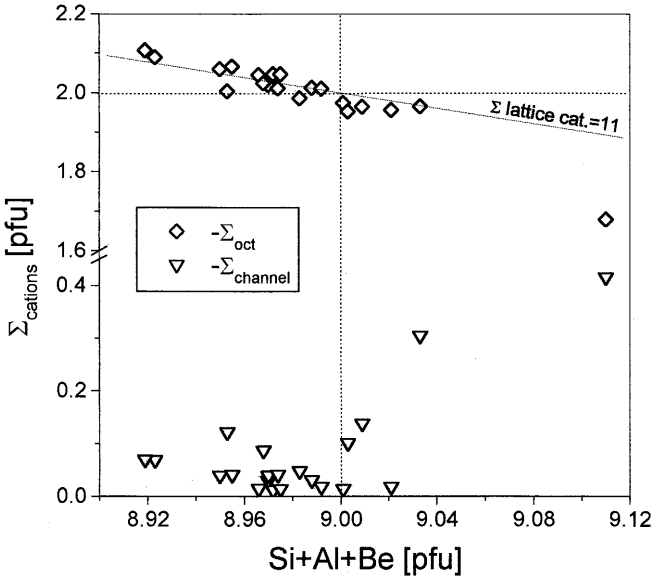

Fig. 3 Sums of the divalent Fe + Mn + Mg cations and channel Na + K + Ca cations versus the sum of the tetrahedral cations

substitutions (2) and/or (3) with a constant sum of 11 lattice cations pfu (Fig. 3). The number of Na, K and Ca channel cations shows, with the exception of two Li, Be-rich samples, a negative correlation versus the total charge of all the lattice cations (Fig. 4), but does not show any correlation versus the sum of the tetrahedral ions. The latter relationship changes its slope at the "stoichiometric" point, from being negative, when there is a tetrahedral cation deficiency, to positive in the case where (Al + Si + Be) > 9 (Fig. 3). These results allow us to determine the importance of substitutions (2) and/or (3) and, therefore, about minor amounts of divalent ions on tetrahedral sites rather than the presence of tetrahedral vacancies in the case where (Al + Si + Be) < 9. From the rough trend shown in Fig. 2, it can be concluded that Fe^{2+} enters about one third of the tetrahedra that are not occupied by Al, Si or Be. The channel cations compensate for the charge deficiency resulting from substitution (2), when (Al + Si + Be) < 9, and by the incorporation of tetrahedral Be and/or octahedral Li when (Al + Si + Be) > 9.

Magnesian cordierites with $X_{Fe} = Fe/(Fe + Mg) < 0.3$ are typically characterized by slightly lower Al contents and there exists a slight positive correlation between X_{Fe} and Al. In ferrous-rich samples, the number of Al cations is close to the stoichiometric number of 4 atoms pfu, with only one exception (Fig. 5). This difference between Mg-rich and more Fe-rich cordierites may reflect an inverse relationship that exists between the mean $T_1$1–O bond length and the mean radius of the octahedral cation (Armbruster 1985). It could explain also why there is more tetrahedral Fe^{2+} in Mg-rich cordierites versus that in Fe-rich samples. In agreement with this, an analysis of the literature data shows a negative correlation between the mean octahedral Me–O distance and the mean T–O distances in the ring-connecting tetrahedra in the structure of double-ring silicates (Bakakin et al. 1975; Cerný et al. 1980; Szymanski et al. 1982; Abraham et al. 1983; Alietti et al. 1994; Armbruster and Oberhänsli 1988a, 1988b; Hawthorne et al. 1991). This reflects a tendency to achieve mutual size compensation between the edge-shared polyhedra.

The presence of small amounts of tetrahedral Fe^{2+}, even in samples which have enough (Al + Si + Be) to fill all tetrahedral sites (Table 2, Fig. 2), demonstrates a slight disorder of Al and (Fe, Mg) between tetrahedral and octahedral sites. Such disorder is common in structurally similar silicates such as osumilite (e.g. Armbruster and Oberhansli 1988a).

Room-temperature single-crystal electronic absorption spectra: absorption bands caused by octahedral and non-octahedral Fe^{2+} ions.

Typical polarized electronic absorption spectra of cordierite are shown in Fig. 6. The Fe^{2+} ions give rise to a doublet consisting of two overlapping bands, v_1 and v_2, located between 11,000 and 8,000 cm^{-1} in the α-polarized

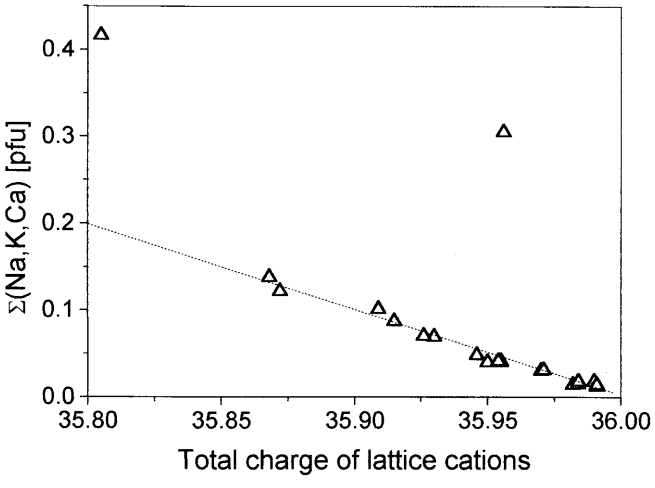

Fig. 4 Channel cation sum as a function of the total charge of the lattice cations

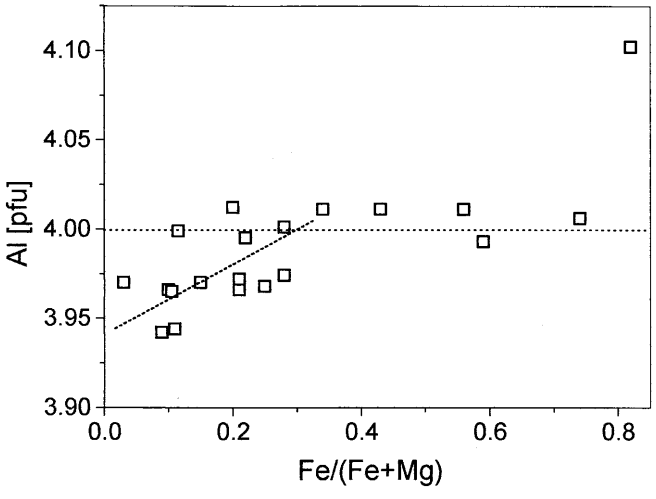

Fig. 5 Plot of the number of aluminium cations versus the Fe/(Fe + Mg) ratio

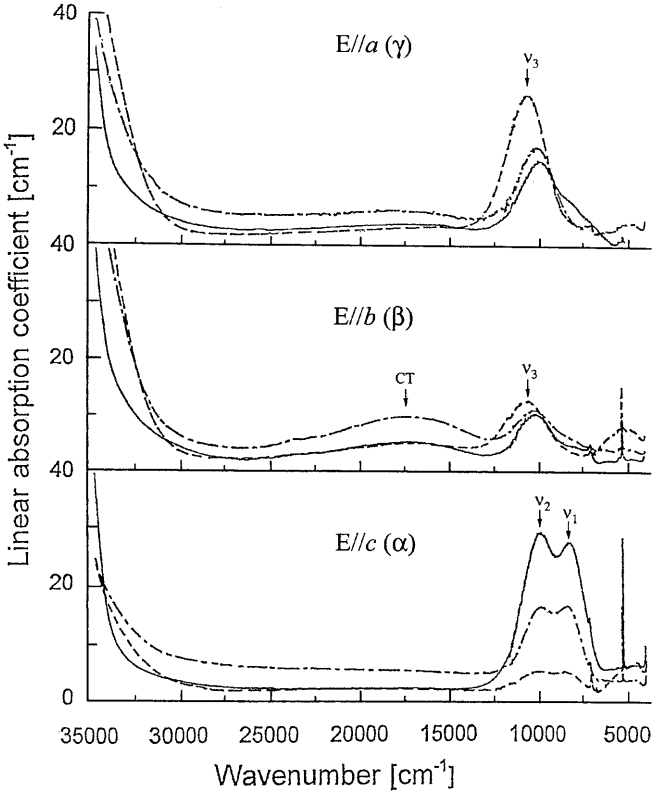

Fig. 6 Room-temperature polarized electronic absorption spectra of cordierites 8c6b/004 (no. 5), *dash lines*; 9–81 (no. 17), *dash–dot lines*; and sekaninaite (no. 21), *solid lines*. *a*, *b*, and *c* are the crystallographic directions

spectra (E//*c*), and a strong, single v_3 band near 10,500 cm^{-1} in the γ- and β-polarized spectra. In the β- and γ-polarized spectra of ferrous-rich cordierites a shoulder at 8,000 cm^{-1} is observed on the low-energy wing of the 10,500-cm^{-1}-centred band (Fig. 6, sekaninaite spectra). Its position and correlation with the intensity of the doublet in the α-polarized spectra support the proposal of Goldman et al. (1977) that it represents a component of a non-fully polarized low-energy v_1 band of the doublet, which is most intense in the α-spectra. The energies of all three bands decrease with increasing total iron content. The bands shift by –300 (v_1), –500 (v_2) and –900 cm^{-1} (v_3) over the compositional range 0.06–1.54 Fe^{2+} pfu (Table 3, Fig. 7a). The integral intensities of the doublet ($A_1 + A_2$), and each of its two bands, are proportional to the total Fe content, while the intensity of the v_3 band shows no such correlation (Fig. 7b).

Results of the spectra deconvolution give a constant ratio of $A_2{:}A_1 \approx 2$ between the integral intensities of the two components of the α-polarized doublet over different Fe/Fe + Mg ratios. The half-widths of the v_1 and v_2 bands are $2{,}000 \pm 400$ cm^{-1} and they show no relationship to composition. The v_1 band at 8,000 cm^{-1} is narrower than the v_2 and v_3 bands centred near 10,000 cm^{-1}. These results are consistent with the assignment of the α-polarized doublet to the spin-allowed transitions of octahedrally coordinated Fe^{2+} derived from the $^5T_{2g} \rightarrow {}^5E_g$ transition in an O_h-symmetry field (Goldman et al. 1977).

X-ray diffraction results define a point symmetry *2* for the octahedral 8*g* site with a twofold axis parallel to *a* (Fig. 1a). This symmetry completely removes the de-

Table 3 Energies (v, cm^{-1}), half-widths (hw, cm^{-1}) and integral intensities (A, cm^{-2}) of electronic absorption bands in the polarized spectra of the cordierite samples measured at room temperature. Errors are estimated to be less than 1% for the energies, and less than 10% for their half-widths and integral intensities. *n.m.* denotes no spectra were measured. *Dash* indicates that no CT bands were observed

Sample no.	E//*c* (α-polarization)						E//*b* (β-polarization)						E//*a* (γ-polarization)		
	v_1	A_1	hw_1	v_2	A_2	hw_2	v_3	A_3	hw_3	v_{CT}	A_{CT}	hw_{CT}	v_3	A_3	hw_3
1	8,480	1,000	1,090	10,160	2,250	1,870	10,840	4,540	2,240	–	–	–	10,820	9,440	2,210
2	8,490	4,510	1,830	10,290	6,700	2,210	10,730	21,120	2,260	–	–	–	10,760	60,260	2,270
3	8,340	3,150	1,460	10,160	7,280	2,190	10,740	24,500	2,450	17,350	17,420	7,320	n.m.	n.m.	n.m.
4	8,400	5,340	1,560	10,110	10,760	2,270	10,580	31,450	2,280	–	–	–	n.m.	n.m.	n.m.
5	8,450	5,020	1,280	10,280	9,720	2,610	10,830	33,260	2,680	17,480	26,600	8,210	10,990	64,490	2,450
6	8,340	3,590	1,140	10,050	7,430	1,960	10,690	15,260	2,020	17,200	27,260	6,610	10,750	36,090	2,060
7	8,430	5,000	1,440	10,190	9,440	2,300	10,680	15,080	2,380	17,430	37,610	7,320	10,770	30,060	2,470
8	8,330	5,050	1,400	10,030	8,220	2,060	10,030	3,570	1,800	–	–	–	10,110	7,380	1,920
9	8,250	10,160	1,740	10,180	18,570	2,310	10,570	28,280	2,440	–	–	–	10,640	55,570	2,410
10	8,340	8,290	1,420	10,050	14,220	2,170	10,070	7,850	2,590	15,870	20,230	5,950	10,130	15,390	2,460
11	n.m.	n.m.	n.m.	n.m.	n.m.	n.m.	10,420	4,600	2,200	17,310	26,910	6,280	10,480	5,540	1,950
12	8,300	8,670	1,170	10,000	18,850	1,980	10,120	4,030	2,330	–	–	–	n.m.	n.m.	n.m.
13	8,290	9,900	1,450	10,070	15,860	1,940	10,420	15,930	2,250	–	–	–	10,560	48,480	2,320
14	8,370	10,800	1,480	10,070	13,080	1,790	10,460	6,230	2,160	17,250	10,9,730	6,430	n.m.	n.m.	n.m.
15	8,130	13,800	1,230	9,910	31,170	1,740	10,510	28,140	2,090	–	–	–	10,500	51,480	2,070
16	8,230	11,620	1,120	9,940	30,110	2,120	10,300	5,350	1,740	–	–	–	n.m.	n.m.	n.m.
17	8,200	17,090	1,510	10,040	31,780	2,330	10,270	14,120	2,310	17,680	54,960	7,060	10,360	29,060	2,470
18	8,020	17,060	1,530	9,900	43,150	2,290	10,000	8,420	2,130	17,470	29,540	7,840	9,860	19,190	2,300
19	8,200	32,940	1,310	9,940	33,000	1,460	n.m.	n.m.	n.m.	n.m.	n.m.	n.m.	10,220	15,170	1,680
20	8,200	25,870	1,350	9,920	42,880	2,070	10,230	5,960	1,670	17,420	15,2,830	7,040	10,290	9,300	1,760
21	8,020	28,760	1,550	10,010	49,930	2,370	10,020	15,100	2,080	16,620	54,500	8,910	10,010	26,220	2,190

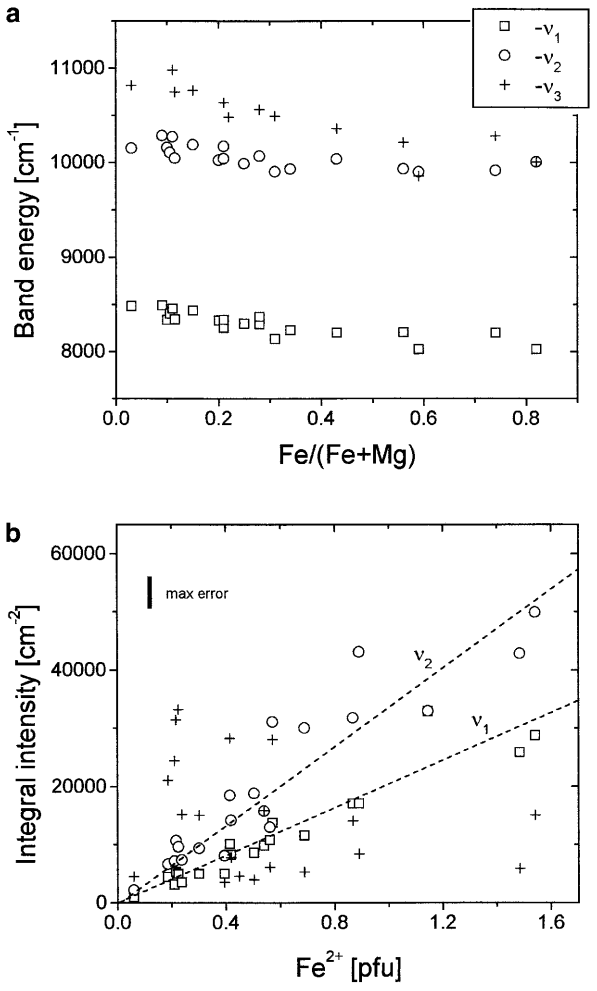

Fig. 7 **a** Energies of the Fe^{2+} absorption bands near 10,000 cm^{-1} as a function of Fe/(Fe+Mg). ν_1 and ν_2 are as fitted from the α-polarized spectra, and ν_3 from the γ-polarized spectra. Errors are equal to or smaller than the symbol size. **b** Integral band intensities versus Fe^{2+} pfu

generacy of the E and T electronic states. As a result, two bands should appear in the electronic absorption spectra due to transitions between the split ground $^5T_{2g}$ and the upper ^5E_g-level, both of which are polarized either parallel or perpendicular to the twofold axis (e.g. Marfunin 1979). In cordierite spectra, however, the doublet is only present in α-polarization (Fig. 6). This could be a result of a pseudo-symmetry higher than *2*, e.g. *3*, with the main trigonal axis parallel to *c*. The higher effective point symmetry gives rise to selection rules and a corresponding polarization of the electronic transitions consistent with the main geometrical distortion of the octahedra, which are strongly compressed along the pseudo-triad axis parallel to *c* (e.g. Gibbs 1966).

A very broad band centred at about 18,000 cm^{-1}, with a β:γ intensity ratio of 2.6–2.9, is often present in the β- and γ-polarized spectra of cordierite (Fig. 6). Its intensity differs strongly between the samples, showing no correlation with the total Fe content, nor with the intensities of the Fe^{2+} bands between 11,000 and 8,000 cm^{-1}. Because it shows all the characteristics of a CT absorption band, i.e. a large half band width of 6,000–8,000 cm^{-1}, energy, thermal behaviour and polarization, it was assigned to $Fe^{2+}Fe^{3+}$ CT (Faye et al. 1968; Smith and Strens 1976; Goldman et al. 1977). However, there is no consensus concerning where the corresponding iron ions reside. Several weak and narrow absorption peaks are superimposed upon the CT band; the most prominent of them are located at about 20,300, 22,700, 23,800 and 25,000 cm^{-1} (Figs. 6, 8). Their energies, intensities and widths are typical of quintet–triplet spin-forbidden Fe^{2+} bands as observed in the spectra of other silicates (e.g. Langer and Abu-Eid 1977; Khomenko and Platonov 1987).

The electronic absorption spectroscopic results are summarized in Table 3. The accuracy of the band parameters depends on the curve-fitting procedures adopted, especially on the background used in the fitting. In the case here (Geiger et al. 2000a), errors are estimated to be less than 1% for the band positions and less than 10% for their half-widths and integral intensities.

Sharp, intense bands, related to internal vibrations of molecular H_2O, are observed between 3,000 and 4,000 cm^{-1}. They are superimposed on a weak and broad absorption feature located between 4,000 and 6,000 cm^{-1}, which is a single band or a band envelope, whose position and polarization cannot be precisely defined due to the strong deformation caused by the intense H_2O stretching bands. Its energy, its correlation in intensity with the β/γ-polarized ν_3 band at 10,500 cm^{-1} and its polarization were given as evidence for minor channel Fe^{2+} (Goldman et al. 1977). This feature was analysed after the H_2O bands were subtracted from the spectra. However, no reasonable quantitative information on band energy, half-width and intensity could be obtained.

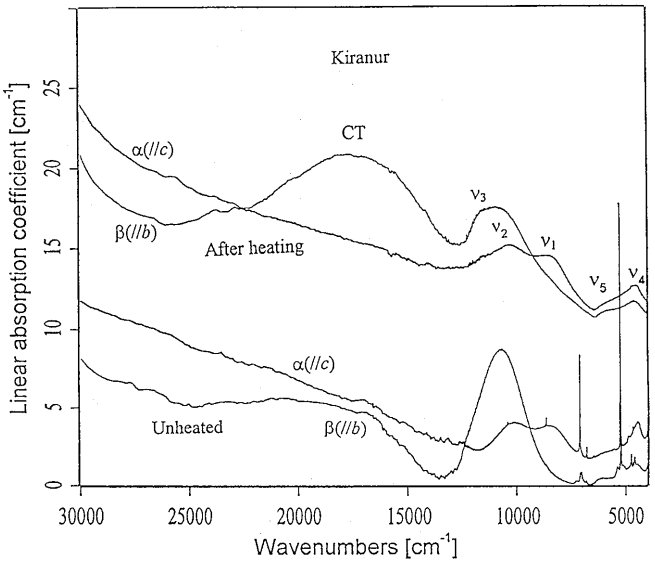

Fig. 8 α- and β-polarized electronic absorption spectra of the Kiranur (no. 3) cordierite before and after heating in air at 1,000 °C for 10 h

In contrast to the data of Goldman et al. (1977), most spectra show the presence of two weak bands in this region: a v_4 band at 4,500–5,000 cm^{-1}, predominantly α-polarized, and a v_5 band at 6,000 cm^{-1}, predominantly β-polarized. The more intense v_4 band occurs at higher energies in iron-rich samples, whereas the v_5 band does not show any change in its spectral position. The intensities of both resolved bands correlate neither with those of the v_3 band at 10,500 cm^{-1}, nor with the α-polarized v_1, v_2 doublet.

To get more information on this weak absorption feature, one crystal of the Kiranur cordierite (no. 3 in Table 1) was heated in air at 1,000 °C for 10 h and then quenched, and its electronic spectra were measured. Its spectra before and after heating are compared in Fig. 8. Because dehydration occurs at 800 °C (e.g. Goldman et al. 1977; Vance and Price 1984), the spectra of the heated sample do not show any H_2O bands and the two-band structure of the envelope at 5,000 cm^{-1} is observed more clearly. The intensity of the v_3 band decreases by a factor of about three upon heating, while no changes can be observed in the intensities of the α-polarized doublet at 10,000 cm^{-1} or the two bands near 5,000 cm^{-1} (Fig. 8). Since Fe^{2+} is the only transition metal ion which can be responsible for absorption in the infrared region, and the energies of both bands near 5,000 cm^{-1} are too high for transitions between the levels derived from the split lower T-state of Fe^{2+} in octahedra (e.g. Langer and Khomenko 1999), a possible explanation for their origin is through the presence of a minor Fe^{2+} fraction in a non-octahedral position.

The existence of the v_3 band after complete dehydration is at odds with the proposal of non-octahedral channel Fe^{2+} that has the oxygen of the water molecule as a ligand. The fivefold channel site (Duncan and Johnston 1974) or the site that includes the six oxygen atoms in the tetrahedral rings, plus one or two overlying and/or underlying oxygens of channel water (Fig. 1b, c), would be destroyed during dehydration. In both of these cases, any corresponding non-octahedral Fe^{2+} would experience a change in its coordination. Therefore, the v_3 absorption band should disappear and new bands at other energies and with other polarizations should arise in the spectra after heating. This, however, does not occur (Fig. 8). The same arguments lead to the conclusion that the weak v_4 and v_5 bands also originate from Fe^{2+} ions which have no water in their first coordination sphere. Because of their weakness and an uncertainty of their intensities, it is difficult to determine their relationship with the non-octahedral Fe^{2+} which gives rise to the strong v_3 band.

Electronic absorption spectra measured at low and high temperatures: local structural characterization of the sites occupied by Fe^{2+}

The electronic absorption bands behave differently upon heating from 80 to 700 K depending upon the nature and the local symmetry of the corresponding structural sites. Generally, with increasing temperature all three bands in the 10,000 cm^{-1} region show changes that are typical of Fe^{2+} *dd* bands: that is a broadening, shifts to lower energies and, in the case of the v_1 and v_2 bands, an increase of integral intensities (Fig. 9, Table 4). The bands of octahedral Fe^{2+} shift to lower energies, with the v_1 band showing a larger T-dependence (ca. –1 cm^{-1} $grad^{-1}$) than the v_2 band (Fig. 10a). This can be related to changes in the structure following heating, since the energies of the v_1 and v_2 bands are determined by the crystal field parameter Dq and the E-state splitting values (Fig. 10b); both the latter are related to the geometry of the structural site containing Fe^{2+} (e.g. Burns 1993). A decrease in Dq, which is related to an increase in the Fe^{2+}–O distances, causes a shift to lower energies of both bands that are derived from the ^{5}E-state, while an increase of the ^{5}E-state split causes the similar effect on the lower level, but moves the upper level to the higher energies. Together, both effects lead to a strong negative temperature dependence of the v_1 band and only minor changes of the v_2 band position (Fig. 10).

The spectra show that Dq decreases with increasing temperature by the same amount –0.05 cm^{-1} $grad^{-1}$ in ferrous and Mg-rich cordierites (Fig. 10b). We calculate

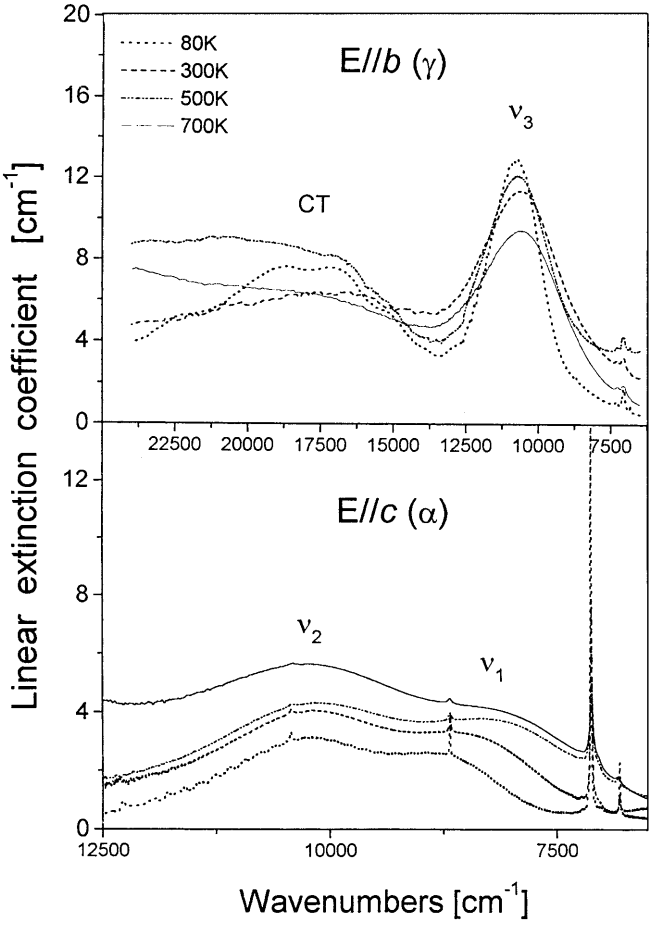

Fig. 9 Polarized electronic absorption spectra of Kiranur (no. 3) cordierite measured at different temperatures

Table 4 Results of optical spectroscopic measurements at different temperatures. Errors are estimated to be less than 1% for the band energies and less than 10% for their half-width and integral intensities. *Dashes* denote no spectra were measured under correspondent conditions, or bands were not observed

Sample no.	T (K)	v_1 Band (α-Polarization)			v_2 Band (α-Polarization)			v_3 Band (β-Polarization)			v_3 Band (γ-Polarization)			CT band (β-polarization)		
		v (cm^{-1})	A (cm^{-2})	hw (cm^{-1})	v (cm^{-1})	A (cm^{-2})	hw (cm^{-1})	v (cm^{-1})	A (cm^{-2})	hw (cm^{-1})	v (cm^{-1})	A (cm^{-2})	hw (cm^{-1})	v (cm^{-1})	A (cm^{-2})	hw (cm^{-1})
3	80	8,630	1,610	1,050	10,190	5,660	2,100	10,770	23,290	1,990	–	–	–	17,760	39,170	6,740
	300	8,340	3,150	1,460	10,160	7,280	2,190	10,740	24,500	2,450	–	–	–	17,350	17,420	7,320
	500	8,050	3,990	1,640	10,130	7,550	2,350	10,590	21,880	2,810	–	–	–	17,050	21,000	7,650
	700	7,950	4,250	1,900	10,080	6,080	2,160	10,520	19,410	2,880	–	–	–	17,080	15,030	8,880
9	80	8,560	3,660	1,070	10,070	14,410	2,270	10,690	27,430	2,010	10,720	53,890	1,950	–	–	–
	300	8,250	10,160	1,740	10,180	18,570	2,310	10,570	28,280	2,440	10,640	55,570	2,410	–	–	–
	500	8,020	10,770	1,850	10,090	14,170	2,160	10,430	22,630	2,580	10,500	50,030	2,660	–	–	–
	700	7,810	9,470	1,810	10,020	16,810	2,450	–	–	–	10,430	44,440	2,710	–	–	–
14	80	–	–	–	–	–	–	–	–	–	–	–	–	17,730	13,5,270	7,030
	300	8,370	10,800	1,480	10,070	13,080	1,790	10,460	6,230	2,160	–	–	–	17,250	10,9,730	6,430
	500	–	–	–	–	–	–	–	–	–	–	–	–	17,530	74,830	6,730
	700	–	–	–	–	–	–	–	–	–	–	–	–	17,450	37,770	5,830
17	80	8,520	9,910	1,180	10,010	21,200	1,940	10,300	13,310	2,050	10,400	34,720	2,350	–	–	–
	300	8,200	17,090	1,510	10,040	31,780	2,330	10,270	14,120	2,310	10,360	29,060	2,470	17,680	54,960	7,060
	500	7,930	21,290	1,720	9,970	36,680	2,470	10,090	15,660	2,380	10,210	36,000	2,920	–	–	–
	700	7,840	25,640	1,850	10,110	38,230	2,500	10,110	16,130	2,470	10,100	26,170	2,630	–	–	–
21	80	8,230	24,550	1,420	9,990	39,340	2,110	10,010	15,180	2,030	9,990	23,670	2,060	16,570	73,900	10,250
	300	8,020	28,760	1,550	10,010	49,930	2,370	10,020	15,100	2,080	10,010	26,220	2,190	16,620	54,500	8,910
	500	7,750	42,630	1,770	9,960	64,480	2,550	9,960	26,910	2,600	9,960	39,500	2,800	17,370	35,510	7,910
	700	7,630	43,790	1,820	9,910	74,220	2,760	9,920	26,450	2,630	10,070	40,710	2,900	17,350	26,340	9,530

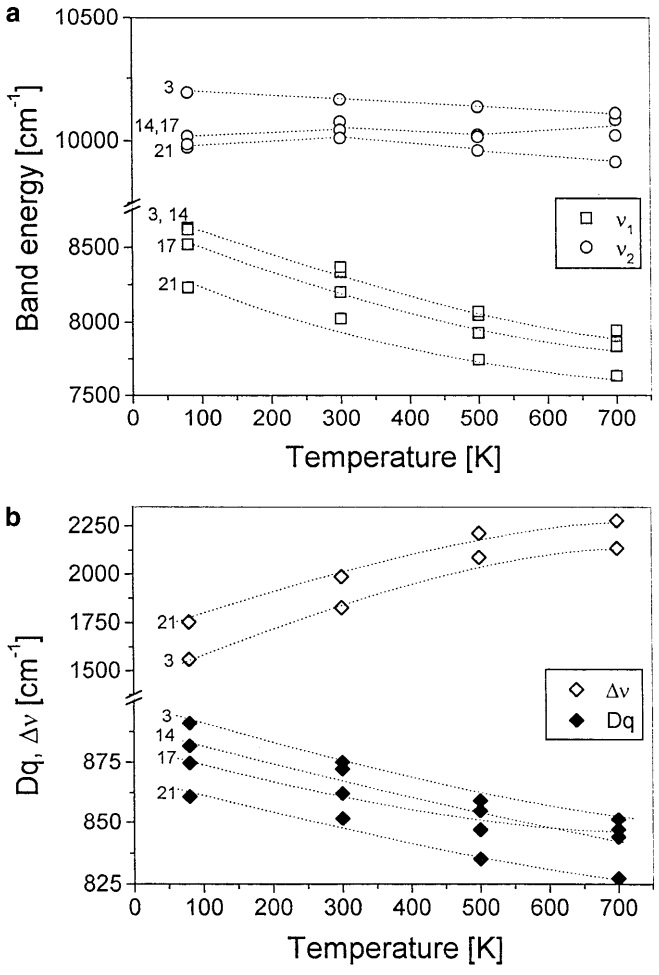

Fig. 10 Temperature change of the absorption doublet consisting of the v_1 and v_2 bands that are related to Fe^{2+} ions in the octahedral site: **a** band energies; **b** crystal field parameter Dq and the ^5E_g-level splitting given as Δv. *Sample numbers* correspond to the numbers in the tables

a mean local Fe^{VI}–O thermal expansion of 12.8×10^{-6} $grad^{-1}$ using the local Me–O distance obtained from 10Dq values (e.g. Langer 2001) and the results obtained from the ferrous-rich sekaninaite (sample no. 21) as a reference. This value is larger than the average octahedral thermal expansion of 9.3×10^{-6} $grad^{-1}$ determined from a high-temperature X-ray structure refinement on sekaninaite and it corresponds better to that of a magnesian-rich cordierite (12.6×10^{-6} $grad^{-1}$) (Hochella et al. 1979). The same local Fe^{VI}–O thermal expansion value was determined for all cordierites regardless of their Fe/(Fe + Mg) ratios.

The temperature dependence of the v_3 absorption band is similar to that of the v_2 band showing a slight shift to lower energies with increasing temperature. This is probably related to an increase in the tetrahedral Fe^{2+}–O bond lengths. The possible lower energy v_4 and v_5 components of the exited T electronic state of tetrahedral Fe^{2+} were not resolved in the high- and low-temperature spectra.

The integral intensities of the v_1 and v_2 bands increase linearly and nearly double upon heating from 80 to 700 K (Fig. 11a). This behaviour is typical for spin-allowed *dd* bands in centrosymmetric crystal fields (e.g. Taran et al. 1994), but can also occur in fields which are slightly distorted from centrosymmetry. It is caused by a weakening of the Laporte selection rules due to a dynamic loss of the symmetry centre $\bar{1}$ at the $3d^N$-ion site at elevated temperatures. On the other hand, the intensity of the v_3 band is nearly independent of temperature (Fig. 11b). This is evidence that the related Fe^{2+} ions are located in a non-centrosymmetric crystal field. This is contradictory to the assignment of the v_3 band to Fe^{2+} in a centrosymmetric channel position (Goldman et al. 1977) and strengthens the arguments given by Vance and Price (1984) and Geiger et al. (2000a) for tetrahedrally coordinated Fe^{2+} ions.

An increase in temperature generates increased thermal motion of an atom that is recorded in the isotropic temperature factor B_{eq} of a diffraction experiment. In

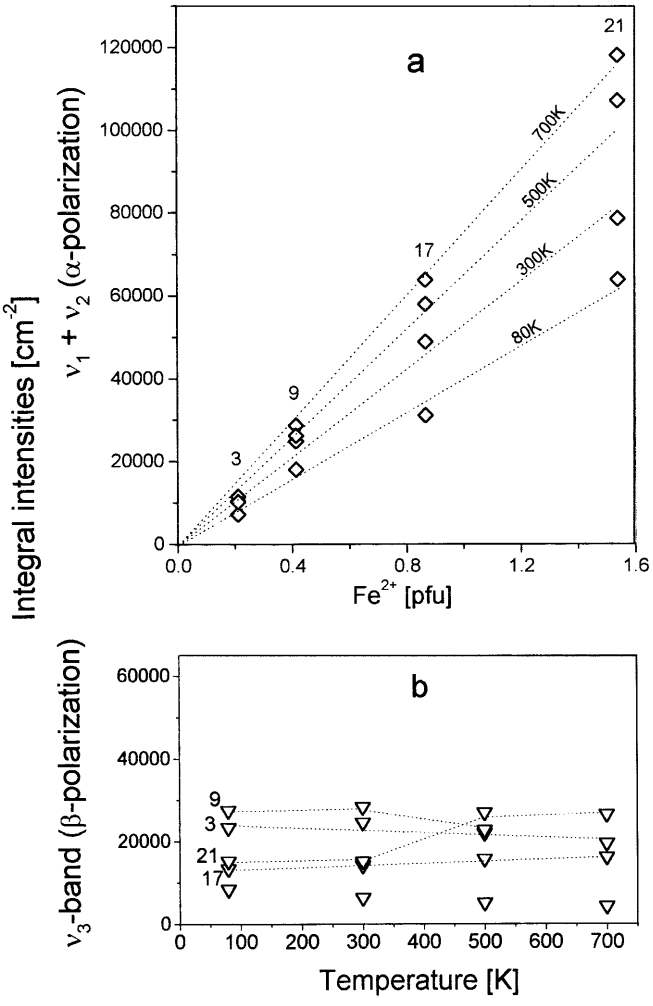

Fig. 11 The temperature dependence of the integral intensity of the Fe^{2+} absorption bands. **a** The v_1 and v_2 bands that are related to octahedrally coordinated Fe^{2+}; **b** the v_3 band related to non-octahedral Fe^{2+} (β-polarization)

electronic spectra, increased thermal motion is reflected by an increase in the widths of the *dd* bands related to the $3d^N$-ions. Indeed, the half-width of the ν_3 band shows a good positive correlation with the B_{eq} values of the tetrahedral $T_1$1 site (Fig. 12). This behaviour is similar to that of the half-widths of the ν_2 band and the B_{eq} values of the octahedral site. The octahedron in cordierite shares two edges with $T_1$1-tetrahedra (Fig. 1). The good correlation between the half-widths of the ν_3 bands and the B_{eq} values for the $T_1$1 site over a range of cordierite compositions is a strong argument in favour of Fe^{2+} on $T_1$1. This is, moreover, consistent with a strongly bonded lattice position for the non-octahedral Fe^{2+} determined on the basis of its Debye temperatures (Vance and Price 1984).

The $Fe^{2+}Fe^{3+}$ CT band at 18,000 cm^{-1}, unlike the *dd* bands, shows a pronounced decrease in its integral intensity and only slight changes in energy upon heating (Fig. 13, Table 4). This is typical for CT bands (e.g. Smith 1977; Taran and Langer 1998). Spectra obtained on three samples show that the CT band intensity decreases by about one third over the temperature interval 80–700 K. This is in agreement with the data reported for cordierite by Taran and Langer (1998).

^{57}Fe Mössbauer results and their correlation with the electronic absorption spectra: concentrations of the non-octahedral Fe^{2+}

The ^{57}Fe Mössbauer spectra of many natural cordierites display a single Fe^{2+} doublet with an isomer shift of 1.31 ± 0.01 mm s^{-1} at 77 K. This doublet can be assigned to octahedrally coordinated Fe^{2+} ions (Duncan and Johnston 1974; Goldman et al. 1977; Geiger et al. 2000a). However, in the spectra of some Mg-rich cordierites, with X_{Fe} below 0.3, two distinct absorption doublets can be observed, thus showing that Fe^{2+} is located on two different structural sites. Similar results were reported before and the assignment of the second smaller doublet has been debated (Duncan and Johnston 1974; Pollak 1976; Goldman et al. 1977; Vance and Price 1984; Geiger et al. 2000a). No measurable ferric iron doublets were detected in the Mössbauer spectra herein. Therefore, the Fe^{3+} content in these cordierites cannot be more than about 2–3% of the total iron.

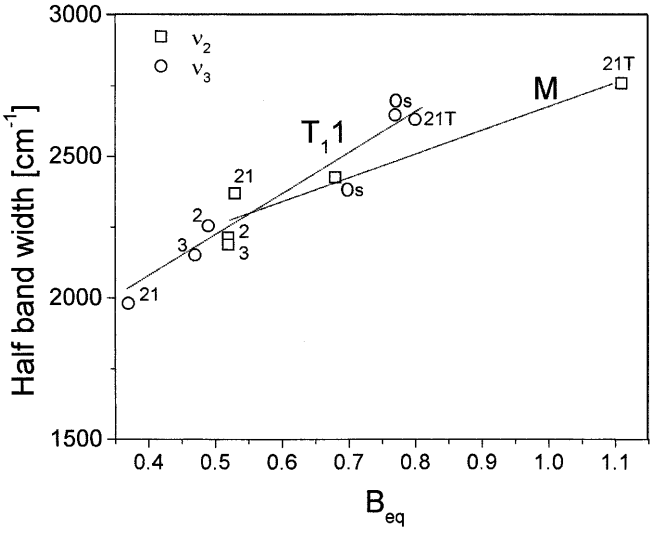

Fig. 12 Half-widths of the Fe^{2+} absorption bands as a function of the isotropic temperature factors, B_{eq}, of the cations in the $T_1$1-tetrahedral and M octahedral positions. The *sample numbers* correspond to numbers in the tables. *Os* osumilite (Armbruster and Oberhänsli 1988a), *21 T* sekaninaite (no. 21) at 650 K (Hochella et al. 1979). Other structural data were taken from Geiger et al. 2000a (nos. 2, 3) and Hochella et al. 1979 (no. 21)

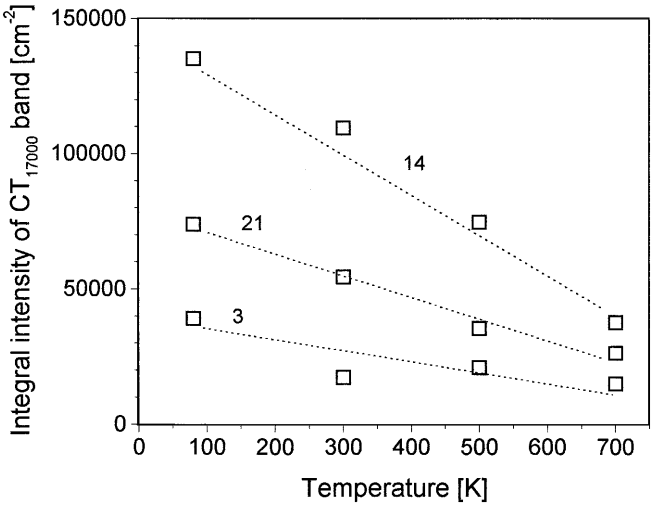

Fig. 13 The temperature behaviour of the integral intensity of $Fe^{2+}Fe^{3+}$ CT band (β-polarization)

The hyperfine parameters from the MS spectra are listed in Table 5. The effect of temperature, 298 vs. 77 K, is very slight: generally, the area of the smaller doublet increases by only a couple of percentage points at 77 K. Typical spectra are shown in Geiger et al. (2000a). From the known total iron contents and the results of the Mössbauer spectra, the octahedral and non-octahedral Fe^{2+} fractions were calculated (Table 6). Figure 14 shows that a linear correlation exists between the amount of non-octahedral Fe^{2+} as determined from the Mössbauer spectra and the integral intensity of the ν_3 band at 10,500 cm^{-1}. This indicates that both originate from Fe^{2+} ions occupying the same structural site. This relationship is used for estimating the non-octahedral Fe^{2+} amounts for all the cordierites studied here. They vary from 0.2 to 10% of the total iron (Table 6). It should be stated that the electronic absorption spectra of all cordierite samples show bands related to non-octahedral Fe^{2+}, but only some of them show a corresponding Mössbauer doublet. For those samples which show a single Mössbauer doublet, the amounts of non-octahedral Fe^{2+} are less than 3%, which would not be detectable by standard Mössbauer methods.

The amount of non-octahedral ferrous iron decreases exponentially with increasing bulk iron (Fig. 15). This is

Table 5 Measured ^{57}Fe Mössbauer parameters of cordierites studied

Sample no.	X_{Fe}	Temperature (K)	I.S.[ab] (mm s^{-1})	Half-width[b] (mm s^{-1})	Q.S.[b] (mm s^{-1})	Absorption (%)
2	0.09	77	1.30	0.13	2.59	90.2
0.99	0.11	2.25	9.8	3	0.10	77
1.32	0.12	2.64	87.7	0.99	0.13	2.32
12.3	4	0.11	77	1.30	0.13	2.61
93.3	0.98	0.12	2.28	6.7	5	0.11
77	1.31	0.12	2.64	89.7	0.99	0.12
2.33	10.3	6	0.12	293	1.19	0.13
2.33	94.4	0.87	0.13	2.26	5.6	9
0.21	77	1.30	0.15	2.61	95.9	0.92
0.10	2.38	4.1	11	0.22	77	1.31
0.13	2.65	100	12	0.25	293	1.19
0.13	2.33	100	14	0.28	293	1.19
0.14	2.30	100	15	0.30	77	1.32
0.13	2.67	97.0	0.99	0.08	2.38	3.0
16	0.34	293	1.19	0.14	2.31	100
17	0.43	293	1.19	0.14	2.30	100
19	0.56	77	1.31	0.14	2.56	100
20	0.74	77	1.31	0.14	2.55	100
21	0.81	77	1.32	0.14	2.56	100

[a]Relative to Fe metal
[b]Uncertainty ± 0.01

Table 6 Estimated atomic Fe^{2+} and Fe^{3+} amounts and their location

Sample no.	Fe_{total}	$Fe_{non\text{-}oct}$ (Mössbauer)	$Fe^{2+}{}_{tetr}$ (recalculated)[a]	$Fe^{3+}{}_{tetr}{}^{b}$ (recalculated)[a]	$Fe^{2+}{}_{oct}{}^{c}$
1	0.06	–	0.003	0.003	0.054
2	0.19	0.018	0.018	0.003	–
3	0.21	0.021	0.021	0.006	0.183
4	0.22	0.014	0.014	0.003	–
5	0.22	0.023	0.023	0.010	–
6	0.24	0.013	0.013	0.010	–
7	0.30	–	0.010	0.014	0.276
8	0.39	–	0.002	0.003	–
9	0.41	0.017	0.017	0.003	0.390
10	0.42	–	0.005	0.007	–
11	0.45	–	0.002	0.010	–
12	0.50	–	0.003	0.003	–
13	0.54	–	0.016	0.003	0.521
14	0.56	–	0.004	0.039	–
15	0.57	0.017	0.017	0.003	0.550
16	0.69	–	0.003	0.003	–
17	0.87	–	0.009	0.020	–
18	0.89	–	0.006	0.011	–
19	1.15	–	0.005	0.003	1.142
20	1.48	–	0.003	0.052	1.425
21	1.54	–	0.009	0.010	1.521

[a]Clarify section "Results and discussion"
[b]Maximal values calculated for ordered distribution
[c]As Fe_{total}–$Fe^{2+}{}_{tetr}$

consistent with cordierite's crystal-chemical properties (cf. Fig. 5) and explains why a non-octahedral Fe^{2+} doublet is observed in magnesium-rich cordierites only (Geiger et al. 2000a).

Ferric iron in cordierite: its location and an estimation of Fe^{3+}/Fe^{2+} ratios

The more recent published data on cordierite show that the Fe^{3+} amounts are very small (e.g. Schreyer 1985; Geiger et al. 2000b). Earlier studies by Pollak (1976) and Parkin et al. (1977) reported the presence of a weak doublet with an isomer shift of about 0.37 ± 0.02 mm s^{-1} in Mössbauer spectra, which they assigned to Fe^{3+} in tetrahedral coordination.

The variability in the intensity of the $Fe^{2+}Fe^{3+}$ CT band in the electronic spectra obtained herein, even between samples with similar total Fe contents (compare Tables 2 and 3), indicates major differences in the Fe^{3+}/Fe^{2+} ratios of natural cordierites. It is difficult to estimate the Fe^{3+} amounts directly, because the molar absorption

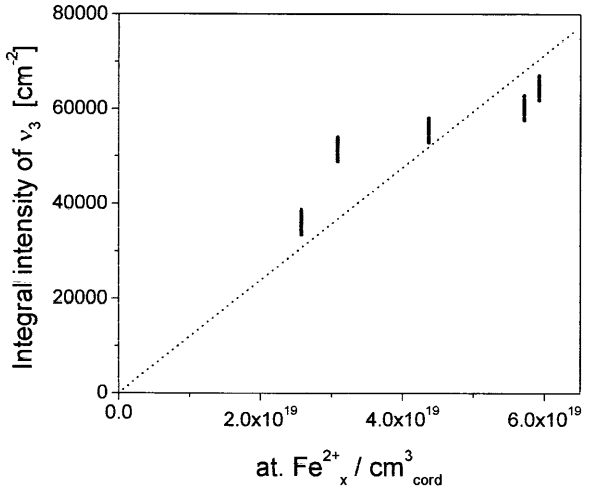

Fig. 14 Integral intensity of the ν_3 band (γ-polarization) versus the concentration of non-octahedral Fe^{2+} as determined by Mössbauer spectroscopy

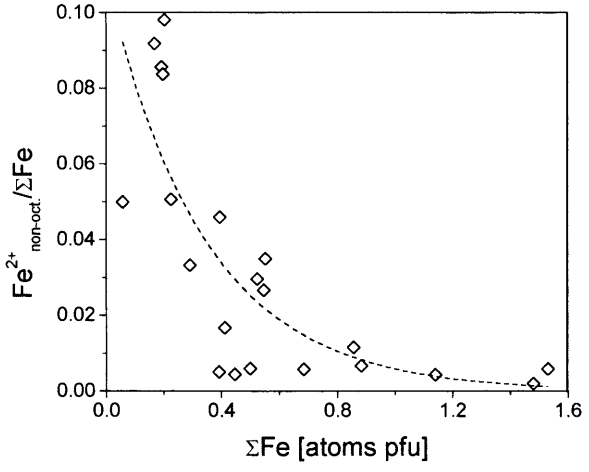

Fig. 15 Mole fraction of non-octahedral Fe^{2+} calculated from the ν_3 band intensities using the correlation from Fig. 14 as a function of total iron

coefficient of the CT band is not known. However, one can make a cautious estimation based on the results of the heating experiments. The CT band near 18,000 cm^{-1} after heating in air increases in intensity, while the ν_3 band at 10,500 cm^{-1} decreases and other Fe^{2+} absorption bands remain unchanged (Fig. 8). Similar observations were interpreted earlier as indicating the oxidation of the non-octahedral Fe^{2+} to Fe^{3+} that then participates in the $Fe^{2+}Fe^{3+}$ CT interaction (Goldman et al. 1977; Vance and Price 1984). Therefore, it is important to note here that the CT band neither changes its energy, nor polarization after heating. This suggests that the Fe^{3+} ions occupy the same structural position before and after heating. Thus, one can estimate the Fe^{3+} contents, if the initial amounts of the non-octahedral Fe^{2+} and the intensities of both the CT and ν_3 bands before and after heating are known. This was done using the Mössbauer data and the electronic spectra obtained on the Kiranur cordierite. It was assumed in a first calculation that all Fe^{3+} ions occupy only sites edge-shared with Fe^{2+}-centred octahedra and, therefore, are involved in the intervalence CT process. In a second calculation, a random distribution of the ferric ions between the same sites, edge-shared with Mg- or Fe^{2+}-centred octahedral, was assumed. The first calculation yields a maximum Fe^{3+} content of 0.006 atoms pfu, whereas the second, more reliable one yields 0.001 atoms pfu. The integral intensities of the CT band were normalized to one Fe^{3+} ion pfu using both models and the Fe^{3+} contents of all the cordierites were determined based on the CT band intensities in their β-polarized spectra. The results give between 0.006 and 0.052 Fe^{3+} pfu for the first model (Table 6) and between 0.001 and 0.01 Fe^{3+} pfu for the second one. These values correspond to 0.5–7% of the total iron in the case of an ordered model or to 0.1–1.5% with a random distribution. In about half of the cordierites studied, the CT band is too weak to be resolved accurately. In these cases its intensity and, therefore, the amount of Fe^{3+} was assumed to be less than half of that in the unheated Kiranur sample. In both cases, the calculated Fe^{3+} amounts in most cordierites are far below the Mössbauer detection limits. No relationship between the Fe^{3+} contents and the bulk chemical composition or geological environment was found. This may be related to low-temperature re-equilibration effects that change the Fe^{3+}/Fe^{2+} ratios.

The polarization of the CT band, which is about $A_{CT}\beta:A_{CT}\gamma = 2.7$, is the same in all the cordierite spectra. It agrees with the theoretically calculated intensity ratio for a CT band caused by an intervalence transition between iron ions located on $T_1$1 and the octahedral site (e.g. Smith and Strens 1976; Goldman et al. 1977). No other pair of edge-shared polyhedra can give this polarization of the CT band. Taking into account that most of the Fe^{2+} is located on the octahedral site, the Fe^{3+} ions must occur on the edge-sharing $T_1$1-tetrahedra. The location of Fe^{3+} on $T_1$1 is supported by single-crystal EPR measurements (Hedgecock and Chakravartty 1966; Geiger et al. 2000b).

Final notes

The number and energy of electronic Fe^{2+} absorption bands in low-symmetry non-octahedral fields

We have shown that neither the temperature behaviour of the ν_3 band, nor its decrease in intensity upon heating connected with the corresponding increase in intensity of the $Fe^{3+,T1}1Fe^{2+,VI}$ CT band, are consistent with an assignment of Fe^{2+} to a channel position. This invalidates the proposal of a six-membered ring channel position (Goldman et al. 1977). If Fe^{2+} occupied such a site, it would have a nearly planar coordination in (001) with possible weaker bonds to H_2O molecules above and below (Fig. 1b). In this case, the number and energy of

absorption bands should be compared to the spectroscopic parameters of Fe^{2+} in a regular planar coordination rather than to those of the distorted non-centrosymmetric M2 position in pyroxene (see Goldman et al. 1977 for the latter).

All the spectroscopic and crystal-chemical results presented here provide evidence supporting the allocation of a minor fraction of Fe^{2+}, as well as a small amount of Fe^{3+}, to the $T_1$1 site. Crystal-chemical arguments and the results of the heating experiments support the proposal that the largest $T_1$1 tetrahedron is the most probable site for most of the non-octahedral Fe^{2+}. This assignment should be consistent with the number, energy and polarization of the observed electronic absorption bands. Therefore, the second and third electronic absorption bands, which must result from the upper split T-level of tetrahedrally coordinated Fe^{2+}, as well as the unusually high energy of the v_3 band, require consideration.

With regards to the number of $Fe^{2+,IV}$ bands, two possibilities should be considered, namely: either the weak v_4 and v_5 bands near 5,000 cm^{-1} are these wanted bands, or they occur between 2,000 and 1,000 cm^{-1}, where they are superimposed by the high-energy wing of the strong lattice vibration bands. In the first case, the corresponding Dq value will be 6,700 cm^{-1}, in the second about 4,000–4,500 cm^{-1}. The latter is typical for tetrahedrally coordinated Fe^{2+} (e.g. Burns 1993), whereas the larger Dq value of 6,700 cm^{-1} is consistent with the $T_1$1–O distances, smaller than in typical ferrous sites. As for the high energy of the T-level splitting, up to 9,000 cm^{-1} in the second case, this is known for $Fe^{2+,IV}$ in other silicates. Gillespite, $BaFeSi_4O_{10}$, for example, contains Fe^{2+} in square-planar coordination, and it shows an energy separation between the two upper levels of about 12,000 cm^{-1} (Abu-Eid et al. 1973). The polarization of the v_3 band in cordierite requires one principal axis of the local crystal field to be parallel to the *c*-axis, which is the case for the $T_1$1 site. Thus, the presence of Fe^{2+} in the large flattened $T_1$1 tetrahedron is consistent with the measured spectroscopic parameters of the v_3 band. An exact interpretation of the two weak bands near 5,000 cm^{-1} remains unclear due to a lack of reliable experimental data. It is likely that the v_4 and v_5 bands are also related to the non-octahedral Fe^{2+} on $T_1$1 site.

Generally, just the number of bands in electronic spectra of different minerals, "typically" three for tetrahedrally coordinated Fe^{2+} or two for Fe^{2+} in octahedral coordination, is not sufficient to assign the absorption bands in the case of low-symmetry non-octahedral fields. There are no straightforward guidelines relating the energy gaps between bands to the site geometry in such cases. For example, the order and energy of electronic levels characteristic of Fe^{2+} in square-planar coordination (Burns 1993) can be regarded as an extreme case of an elongated octahedral or flattened tetrahedral field. In such cases, the polarization dependence of the *dd* and CT bands, their molar absorptivity and thermal behaviour are the most reliable properties related to the site geometry.

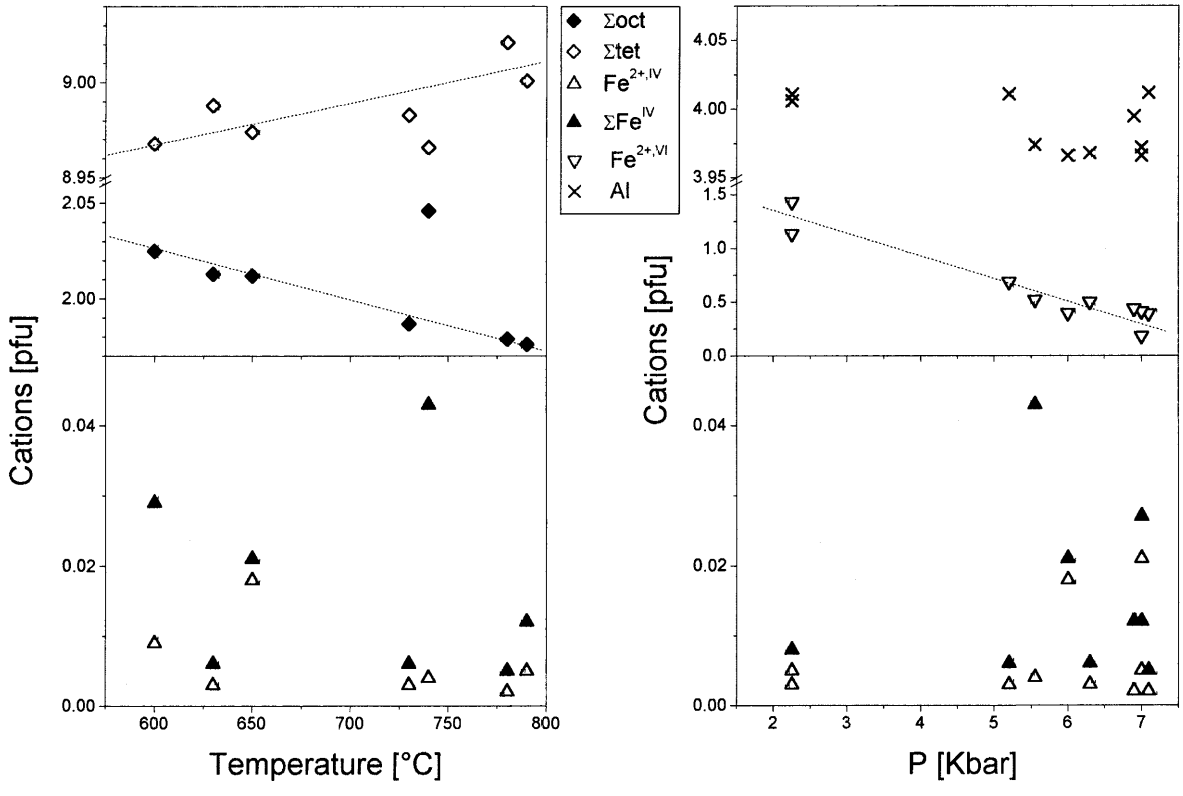

Fig. 16 Compositional variations in cordierite as a function of the temperature determined by garnet–cordierite thermometry **a** and pressure via geobarometry **b**. For sources of the PT data see Table 1

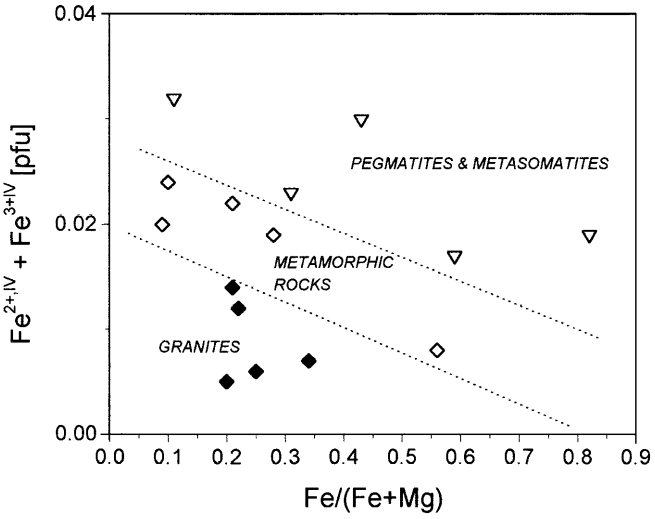

Fig. 17 The Fe/(Fe + Mg) ratio versus the total tetrahedral iron contents in cordierite from different geological environments

Fe^{2+} partitioning in cordierite: petrological relevance?

The amount of Fe^{2+} on the $T_1$1 site depends on the cordierite composition, particularly on the total Fe content (Fig. 15). When coexisting with other ferromagnesian paragenetic minerals such as garnet or biotite, the Fe/Fe + Mg ratio of cordierite is sensitive to the temperature of equilibration (e.g. Aranovich and Podlesskii 1983). The equilibration temperatures for some of the cordierite samples studied here are known from the literature (Table 1), which permit us to investigate the role of $Fe^{2+,IV}$. Linear correlations are observed between the temperature of equilibration and the number of tetrahedral cations (positive) or the sum of the divalent octahedral cations (negative) (Fig. 16a). The amount of $Fe^{2+,IV}$ and the sum of the non-octahedral ferrous and ferric ions, $Fe^{2+,IV} + Fe^{3+,IV}$, show a negative correlation versus temperature (Fig. 16a). Scatter is introduced by experimental errors, as well as by the neglecting the effect of Mg^{IV}, which could also occupy some of the T_1l-tetrahedra.

The molar volume of cordierite depends mainly on the mole fraction of octahedral Fe^{2+} (e.g. Hochella et al. 1979; Wallace and Wenk 1980). This relationship results in a negative linear correlation between pressure of equilibration and $Fe^{2+,VI}$ content (Fig. 16b). A decrease in the total iron content is accompanied by a slight decrease in Al and an increase in Fe^{2+} on $T_1$1 (Fig. 16b). This leads to Fe^{IV} enrichment in cordierites from low-temperature, medium-pressure environments. In plots of X_{Fe} versus Fe^{IV}, the different cordierites can be defined based on a magmatic, metamorphic or pegmatitic origin (Fig. 17). This plot shows that a decrease in tetrahedral Fe^{2+} is related to a temperature increase going from pegmatitic and metamorphic rocks to anatectic granitoids. It can also be seen that $Fe^{2+,IV}$ decreases with increasing total iron content (Fig. 15).

The presence of non-octahedral iron affects the Mg–Fe partitioning relationship between coexisting minerals and should be taken into consideration in geothermometry studies. This effect is illustrated for a magnesian-rich cordierite with a $Fe^{2+,IV}$ content of 0.02 atoms pfu on the basis of Eq. (5) in Kurepin (1991), which produces a change in the calculated temperature of + 50°.

Acknowledgements D. Ackermand, T. Armbruster, S. Herting, V.A. Kurepin, A. Mottana, P. Raase, G.R. Rossman, V. Schenk, A. Speer and D.K. Voznyak generously provided the cordierite samples. F. Galbert, Technical University Berlin, helped with electron microprobe analyses. The German Science Foundation, Bonn-Bad Godesberg, provided research grants to V.M.K. and financial support through Ge 659/6–1 to C.A.G. The optical absorption spectrometers used were made available by the German Science Foundation through La 324/32 to K.L. INTAS, Brussels, contributed generously to the project under 97–32174. To all these individuals and institutions our sincere thanks are due.

References

Abraham K, Gebert W, Medenbach O, Schreyer W, Hentschel G (1983) Eifelite, $KNa_3Mg_4Si_{12}O_{30}$, a new mineral of the osumilite group with octahedral sodium. Contrib Mineral Petrol 82:252–258

Abu-Eid RM, Mao HK, Burns RG (1973) Polarized absorption spectra of gillespite at high pressure. Carnegie Inst Yearb 72:564–567

Alietti E, Brigatti MF, Capedri S, Poppi L (1994) The roedderite–chayesite series from Spanish lamproites: crystal chemical characterization. Mineral Mag 58:655–662

Aranovich LY, Podlesskii KK (1983) The cordierite–garnet sillimanite–quartz equilibrium: experiments and applications. In: Saxena SK (ed) Kinetics and equilibrium in mineral relations. Springer, Berlin Heidelberg New York, pp 173–198

Armbruster T (1985) Fe-rich cordierites from acid volcanic rocks, an optical and x-ray single-crystal structure study. Contrib Mineral Petrol 91:180–187

Armbruster T (1986) Role of Na in the structure of low-cordierite: a single-crystal X-ray study. Am Mineral 71:746–757

Armbruster T, Oberhänsli R (1988a) Crystal chemistry of osumilites. Am Mineral 73:585–594

Armbruster T, Oberhänsli R (1988b) Crystal chemistry of double-ring silicates: structures of sugilite and brannockite. Am Mineral 73:595–600

Bakakin VV, Balko VP, Solovyeva LP (1975) Crystal structures of milarite, armenite and sogdianite. Sov Phys Cryst 19:460–462

Burns RG (1993) Mineralogical applications of crystal field theory, 2nd edn. Cambridge Univ Press, Cambridge

Cerný P, Hawthorne FC, Jarosewich E (1980) Crystal chemistry of milarite. Can Mineral 18:41–57

Cerný P, Chapman R, Schreyer W, Ottolini L, Bottazzi P, McCammon CA (1997) Lithium in sekaninaite from the type locality, Dolni Bory, Czech Republic. Can Mineral 35:167–173

Duncan JF, Johnston JH (1974) Single-crystal ^{57}Fe Mössbauer studies of the site positions in cordierite. Aust J Chem 27:249–258

Faye GH, Manning PG, Nickel EH (1968) The polarized optical absorption spectra of tourmaline, cordierite, chloritoid and vivianite: ferric–ferrous electron interaction as a source of pleochroism. Am Mineral 53:1174–1201

Geiger CA, Armbruster T, Khomenko V, Quartieri S (2000a) Cordierite I: the role of Fe^{2+}. Am Mineral 85:1255–1264

Geiger CA, Rager H, Czank M. (2000b) Cordierite III: the site occupation and concentration of Fe^{3+}. Contrib Mineral Petrol 140:344–352

Gibbs GV (1966) The polymorphism of cordierite I: the crystal structure of low cordierite. Am Mineral 51:1068–1087
Goldman DS, Rossman GR, Dollase WA (1977) Channel constituents in cordierite. Am Mineral 62:1144–1157
Hawthorne FC, Kimata M, Cerný P, Ball N, Rossman GR, Grice JD (1991) The crystal chemistry of the milarite-group minerals. Am Mineral 76:1836–1856
Hedgecock NE, Chakravartty SC (1966) Electron spin resonance of Fe^{3+} in cordierite. Can J Phys 44:2749–2755
Hochella MFJ, Brown GEJ, Ross FK, Gibbs GV (1979) High-temperature crystal chemistry of hydrous Mg- and Fe-cordierites. Am Mineral 64:337–351
Khomenko VM, Platonov AN (1987) Rock-forming pyroxenes: optical spectra, colour and pleochroism (in Russian). Naukova Dumka, Kiev
Khomenko VM, Langer K, Andrut M, Koch-Müller M, Vishnevsky AA (1994) Single crystal absorption spectra of synthetic Ti, Fe-substituted pyropes. Phys Chem Miner 21:434–440
Kurepin VA (1991) Thermodynamic conditions of the formation of the garnet–cordierite–biotite association in the Berdichev granite (Ukrainian Shield) (in Russian). Mineral Zh 13(1):76–87
Lal RK, Ackermand D, Raith M, Raase P, Seifert F (1984) Sapphirine-bearing assemblages from Kiranur, Southern India: a study of chemographic relationships in the Na_2O–FeO–MgO–Al_2O_3–SiO_2–H_2O system. Neues Jahrb Mineral 150:121–152
Langer K (1988) UV to NIR spectra of silicate minerals obtained by microscope spectrometry and their use in mineral thermodynamics and kinetics. In: Salje EKH (ed) Physical properties and thermodynamic behaviour of minerals. Reidel, Dordrecht, pp 639–685
Langer K (2001) A note on mean distances, $R_{[MOn]}$ in substituted polyhedra $[(M_{1-x}M'_x)O_n]$, in the crystal structures of oxygen based crystal solid solutions: local versus crystal averaging methods. Z Kristallogr 216 (in press)
Langer K, Abu-Eid RM (1977) Measurement of the polarized absorption spectra of synthetic transition metal-bearing silicate microcrystals in the spectral range 44000–4000 cm^{-1}. Phys Chem Miner 1:273–299
Langer K, Khomenko VM (1999) The influence of crystal field stabilization energy on Fe^{2+} partitioning in paragenetic minerals. Contrib Mineral Petrol 137:220–231
Marfunin AS (1979) Physics of minerals and inorganic materials. Springer, Berlin Heidelberg New York
Mottana A, Fusi A, Potenza BB, Crespi R, Liborio G (1983) Hydrocarbon-bearing cordierite from the Derivo–Colico road tunnel (Como, Italy). Neues Jahrb Mineral 148:181–199
Newton RC (1966) BeO in pegmatitic cordierite. Mineral Mag 35:920–927
Pan Y, Fleet ME (1995) Geochemistry and origin of cordierite–orthoamphibole gneiss and associated rocks at an Archaean volcanogenic massive sulfide camp: Manitouwadge, Ontario, Canada. Precambrian Res 74:73–89
Parkin KM, Loeffler BM, Burns RG (1977) Mössbauer spectra of kyanite, aquamarine, and cordierite showing intervalence charge transfer. Phys Chem Miner 1:301–311
Pollak H (1976) Charge transfer in cordierite. Phys Status Solidi B 74:31–34
Raase P, Schenk V (1994) Petrology of granulite-facies metapelites of the Highland Complex, Sri Lanka: implications for the metamorphic zonation and the P–T path. Precambrian Res 66:265–294
Shannon RD, Mariano AN, Rossman GR (1992) Effect of H_2O and CO_2 on dielectric properties of single-crystal cordierite and comparison with polycrystalline cordierite. J Am Ceram Soc 75(9):2395–2399
Schreyer W (1985) Experimental studies on cation substitutions and fluid incorporation in cordierite. Bull Mineral 108:273–291
Selkregg K, Bloss FD (1980) Cordierites: compositional controls of Δ, cell parameters, and optical properties. Am Mineral 65:522–533
Smith G (1977) Low-temperature optical studies of metal–metal charge-transfer transitions in various minerals. Can Mineral 15:500–507
Smith G, Strens RGJ (1976) Intervalence transfer absorption in some silicate, oxide and phosphate minerals. In: Strens RGJ (ed) The physics and chemistry of minerals and rocks. Wiley, New York, pp 583–612
Speer JA (1982) Metamorphism of the pelitic rocks of the Snyder Group in the contact aureole of the Kiglapait layered intrusion, Labrador: effects of buffering partial pressures of water. Can J Earth Sci 19:1888–1909
Stanek J, Miskovsky J (1964) Iron-rich cordierite from a pegmatite near Dolni Bory, W. Moravia, Czechoslovakia. Casopis Mineral Geol 9:191–192
Szymanski JT, Owens DR, Roberts AC, Ansell HG, Chao GY (1982) A mineralogical study and crystal-structure determination of nonmetamict ekanite, $ThCa_2Si_8O_{20}$. Can Mineral 20:65–75
Taran MN, Langer K (1998) Temperature and pressure dependence of intervalence charge transfer bands in spectra of some Fe- and Fe,Ti-bearing oxygen-based minerals. Neues Jahrb Mineral 172:325–346
Taran MN, Langer K, Platonov AN, Indutny VV (1994) Optical absorption investigation of Cr^{3+} ion-bearing minerals in the temperature range 77–797 K. Phys Chem Miner 21:360–372
Vance ER, Price DC (1984) Heating and radiation effects on optical and Mössbauer spectra of Fe-bearing cordierites. Phys Chem Miner 10:200–208
Voznyak DK, Pavlishin VI, Bugaenko VN, Galaburda YA (1996) Nature, origin and geochronology of radiogenic haloes in minerals of the Polokhivske deposit (Ukrainian Shield) (in Russian). Mineral Zh 18(5):3–17
Wallace JH, Wenk H-R (1980) Structure variation in low cordierites. Am Mineral 65:96–111